IEEE Access
Multidisciplinary | Rapid Review | Open Access Journal

Received December 25, 2019, accepted January 3, 2020, date of publication January 7, 2020, date of current version January 16, 2020.

Digital Object Identifier 10.1109/ACCESS.2020.2964570

Nonlinear Dynamics of Rogue Waves in a Fifth-Order Nonlinear Schrödinger Equation

NI SONG, HUI XUE, AND XIAOYING ZHAO
Department of Mathematics, North University of China, Taiyuan 030051, China

Corresponding author: Ni Song (songni@nuc.edu.cn)

This work was supported in part by the National Natural Science Foundation of China (NSFC) under Grant 11602232, in part by the Shanxi Natural Science Foundation (SNSF) under Grant 201801D221040 and Grant 201801D121158, and in part by the Fund for Shanxi under Grant 1331KIRT.

ABSTRACT In this paper, nonlinear dynamics of higher-order rogue waves are investigated for a fifth-order nonlinear Schrödinger equation, which can be used to depict the Heisenberg ferromagnetic spin chain. A generalized Darboux transformation is constructed based on the Lax pair. Higher-order rogue waves solutions are given in terms of a recursive formula. Using numerical simulation, the first-order to the third-order rogue waves are displayed on the basis of some free parameters, which play a crucial role in affecting the distribution of rogue waves. The results obtained should be useful in understanding the generation mechanism of rogue waves.

INDEX TERMS Darboux transformation, fifth-order nonlinear Schrödinger equation, rogue waves.

I. INTRODUCTION

A rogue wave, known as freak wave, monster wave, giant wave, episodic wave etc., is a rare, short-lived and large-amplitude local wave. It is unexpected and suddenly occurs without any warning which can be extremely dangerous, even to large ships. Rogue waves were firstly found in the deep ocean [1], and then studied in the fields of optics [2]–[4], plasmon [5], super fluids [6], capillary waves [7] and so on. In oceanography, a rogue wave is more precisely defined as a wave whose height is more than twice the significant wave height. It occurs when physical factors such as high winds and strong currents cause waves to merge to create a single exceptionally large wave and can involve spontaneous formation of massive waves far beyond the usual expectations of the ship designers [8]. The existence of a rogue wave has been confirmed by video, photographs, stereo wave imaging system [9], [10] and oceanographic research vessel notably [11]. Because of its serious damage, uncertainty and unpredictability when it happens, a rogue wave has been a hot-spot issue in the aspect of the wave theory and applied research since 2005. However, the biggest difficulty of studying extremely dangerous rogue waves in the ocean is scarcity of actual field measurements. Therefore, the study of rogue waves is mainly focused on the theoretical aspects.

In the ocean and nonlinear optics etc., a lot of mathematical models can be described by nonlinear partial differential equations, which are used to analyze and study rogue waves. One of the important known models is the nonlinear Schrödinger (NLS) equation, which can depict a large number of phenomena and dynamic processes in physics, chemistry, biology and computer science [12], [13]. Many research results have been obtained for the NLS equation [14]–[17]. Peng *et al.* [18] made use of the Riemann-Hilbert formulation getting the multi-soliton solutions of an integrable three-component coupled nonlinear Schrödinger (CNLS) equation. Yan *et al.* [19] investigated higher order rogue wave solutions of The higher order CNLS equation by the Darboux-dressing transformation. Guo *et al.* [20] acquired the multi-soliton solutions and Hirota bilinear form of the Heisenberg ferromagnetic spin chain equation by using a potential transformation. Tian [21], [22] researched the initial boundary value problems of the mixed and general CNLS equation by the Fokas method. Peng *et al.* [23], [24] obtained positon wave, high-order rogue wave and breather solutions of the CNLS equation via DT. Tian and Zhang [25] investigated the long-time asymptotics about the solution for the

The associate editor coordinating the review of this manuscript and approving it for publication was Derek Abbott.

Gerdjikov-Ivanov (GI) type of NLS equation. Other than this, the Hirota equation [26], the Fokas-Leneels equation [27], the Sasa-Satsuma equation [28], the discrete Ablowita-Ladik and Hirota equation [29], the Hirota Maxwell-Bloch (MB) equation [30] and the NLS-MB equation [31] are a few of nonlinear evolution equations that admits rogue waves.

Motivated by the aforementioned works, in this paper, a fifth-order NLS equation from the Heisenberg ferromagnetism will be considered [32]

$$iq_t - i\varepsilon q_{xxxxx} - 10i\varepsilon|q|^2 q_{xxx} - 20i\varepsilon q_x q^* q_{xx} - iq_x - 30i\varepsilon|q|^4 q_x - 10i\varepsilon(|q|^2 q)_x + q_{xx} + 2q|q|^2 = 0, \quad (1)$$

where $q(x, t)$ is a complex function, x and t denote the spatial coordinate and the scaled time, respectively, ε is a perturbation parameter and the asterisk represents the complex conjugation. Equation (1) is generated via the deformation of Heisenberg ferromagnetic system with the prolongation structure in Minkowski space and can be used to describe the dynamics of a site-dependent Heisenberg ferromagnetic spin chain [33], which plays a crucial role in nonlinear waves propagation [34], [35] and information technology [36].

Much research has been done on lower-order NLS equations, including studies on solitons, rogue waves and modulation instability [37]. In [38], the Grammian N-soliton, breather and rogue wave solutions of the cylindrical Kadomtsev-Petviashvili equation were obtained via the novel gauge transformation and long wave limit method. In [39], the bright-dark soliton, rational breather wave, traveling wave and rogue wave solutions for the generalized Kadomtsev-Petviashvili equation were acquired by introducing the extended homoclinic test method and the Riccati equation method. In [40], on the basis of Hirota's direct method, the N-soliton wave, breather wave and rational solutions of the Boiti-Leon-Manna-Pempinelli equation were derived. As for higher-order NLS equations. Yang *et al.* studied breathers and rogue wave of the fifth-order NLS equation in the Heisenberg ferromagnetic spin chain [41]. Sun *et al.* [42] discussed the complex nonlinearities of rogue waves for the fourth-order NLS equation. Song *et al.* [43] derived the one- and two-soliton for the fifth-order NLS equation. Wang *et al.* [44] took advantage of bilinear method and obtained the multiple lump solutions of the $(3 + 1)$-dimensional potential Yu-Toda-Sasa-Fukuyama equation. Zhao and He [45] studied the breather wave and rogue wave solutions by the modified DT and obtained the three-dimensional diagrams for the higher-order NLS equation. Wang *et al.* [46]–[48] derived the quasi-periodic wave, breather and rogue wave solutions for the three-component CNLS equation, nonlinear Fokas equation and the $(2 + 1)$-dimensional NLS equation. However, to the best of our knowledge, there are less work about the plot of higher-order rogue waves of higher-order NLS equation.

The aim of this paper is to construct the Nth-order rogue wave solutions for the fifth-order nonlinear Schrödinger equation by using the generalized Darboux transformation (DT) [49]. Based on the DT matrix, a generalized DT is constructed, and the formula for generating the Nth-order rogue wave solutions are given. Nonlinear dynamics of the first-order to the third-order rogue waves are investigated with the influence of some parameters and a few interesting structures are shown.

II. GENERALIZED DARBOUX TRANSFORMATION

DT is an important tool to construct the Nth-order rogue waves solutions. The Lax pair ensuring the integrability of the fifth-order NLS equation (1) is given as follows [23]

$$\Phi_x = U\Phi = \begin{pmatrix} -i\lambda & q \\ -q^* & i\lambda \end{pmatrix}\Phi, \quad (2a)$$

$$\Phi_t = V\Phi = \begin{pmatrix} A & B \\ -B^* & -A \end{pmatrix}\Phi, \quad (2b)$$

with

$$\begin{aligned} A =& -16i\lambda^5\varepsilon + 8i\lambda^3\varepsilon|q|^2 + 4\lambda^2\varepsilon(qq_x^* - q_x q^*) - 2i\lambda^2 \\ & - 2i\lambda\varepsilon(qq_{xx}^* + q^* q_{xx} - |q_x|^2 + 3|q|^4) - i\lambda + \varepsilon(q^* q_{xxx} \\ & - qq_{xxx}^* + q_x q_{xx}^* - q_{xx}q_x^* + 6|q|^2 q^* q_x - 6|q|^2 q_x^* q) + i|q|^2, \\ B =& 16\lambda^4\varepsilon q + 8i\lambda^3\varepsilon q_x - 4\lambda^2\varepsilon(q_{xx} + 2|q|^2 q) \\ & - 2i\lambda\varepsilon(q_{xxx} + 6|q|^2 q_x) + 2\lambda q + \varepsilon(q_{xxxx} + 8|q|^2 q_{xx} \\ & + 2q^2 q_{xx}^* + 4|q_x|^2 q + 6q_x^2 q^* + 6|q|^4 q) + iq_x + q, \end{aligned}$$

where $\Phi = (\varphi_1, \varphi_2)^T$ is vector eigenfunction of the Lax pair (2a) and (2b), q is a potential function, λ is a spectral parameter and the asterisk denotes the complex conjugate.

Introducing a special gauge transformation

$$\Phi[1] = T\Phi. \quad (3)$$

Construct the Darboux matrix T with the Theorm in Reference [37]

$$T = \lambda I - H\Lambda H^{-1}, \quad (4)$$

where

$$I = \begin{pmatrix} 1 & 0 \\ 0 & 1 \end{pmatrix}, \quad H = \begin{pmatrix} \varphi_1 & -\varphi_2^* \\ \varphi_2 & \varphi_1^* \end{pmatrix}, \quad \Lambda = \begin{pmatrix} \lambda_1 & 0 \\ 0 & \lambda_1^* \end{pmatrix}.$$

We assume that $\Phi = (\varphi_1, \varphi_2)^T$ is an eigenfunction of the Lax pair (2a) and (2b) with a seeding solution $q = q[0]$ and $\lambda = \lambda_1$. It is obvious that $(-\varphi_2^*, \varphi_1^*)^T$ also satisfies equation (2) corresponding to $q = q[0]$ and $\lambda = \lambda_1^*$. Choosing different eigenfunctions $\Phi_k = (\varphi_{1k}, \varphi_{2k})^T$ at λ_k, respectively, the aforementioned DT procedure can be easily iterated.

Using equation (4), the Nth-order DT and rogue wave solution for equation (1) are obtained as

$$\begin{aligned} &\Phi_N[N-1] \\ &\quad = T[N-1]T[N-2]\cdots T[1]T[0]\Phi_N, \quad (5a) \\ &q[N] = q[0] - 2i\sum_{k=1}^{N}(\lambda_1 - \lambda_1^*)\frac{\varphi_{1k}[k-1]\varphi_{2k}^*[k-1]}{|\varphi_{1k}[k-1]|^2 + |\varphi_{2k}[k-1]|^2}, \quad (5b) \end{aligned}$$

where

$$T[k] = \lambda_{k+1} I - H[k-1]\Lambda[k]H[k-1]^{-1},$$
$$H[k-1] = \begin{pmatrix} \varphi_{1k}[k-1] & -\varphi_{2k}^*[k-1] \\ \varphi_{2k}[k-1] & \varphi_{1k}^*[k-1] \end{pmatrix},$$
$$\Lambda[k] = \begin{pmatrix} \lambda_k & 0 \\ 0 & \lambda_k^* \end{pmatrix}.$$

On the basis of the elementary DT, a generalized DT can be constructed for equation (1). Supposing that

$$\Psi = \Phi_1(\lambda_1, \eta)$$

is a special solution of the Lax pair (2a) and (2b), where η is a small parameter. Expanding Ψ in the Taylor series at $\eta = 0$, then

$$\Psi = \Phi_1^{[0]} + \Phi_1^{[1]}\eta + \Phi_1^{[2]}\eta^2 + \cdots + \Phi_1^{[m]}\eta^m + o(\eta^m), \quad (6)$$

where

$$\Phi_1^{[j]} = \frac{1}{j!}\frac{\partial^j}{\partial\lambda^j}\Phi_1(\lambda)|_{\lambda=\lambda_1}, \quad (j = 1, 2, \cdots m).$$

It is easily proved that $\Phi_1^{[0]} = \Phi_1[0]$ is a particular solution of the Lax pair (2a) and (2b) with $q = q[0]$ and $\lambda = \lambda_1$. Then, the Nth-step generalized DT is derived as follows

$$\Phi_1[N-1] = \Phi_1^{[0]} + \left[\sum_{l=1}^{N-1} T_1[l]\right]\Phi_1^{[1]} + \left[\sum_{l=1}^{N-1}\sum_{k>l}^{N-1} T_1[k]T_1[l]\right]\Phi_1^{[2]} + \cdots + [T_1[N-1]T_1[N-2]\cdots T_1[1]]\Phi_1^{[N-1]}, \quad (7)$$

$$q[N] = q[N-1] - 2i(\lambda_1 - \lambda_1^*)\frac{\varphi_1[N-1]\varphi_2^*[N-1]}{|\varphi_1[N-1]|^2 + |\varphi_2[N-1]|^2}, \quad (8)$$

$$T_1[k] = \lambda_1 I - H_1[k-1]\Lambda[1]H_1[k-1]^{-1}, \quad 9(a)$$

$$H_1[k-1] = \begin{pmatrix} \varphi_{1k}[k-1] & -\varphi_{2k}^*[k-1] \\ \varphi_{2k}[k-1] & \varphi_{1k}^*[k-1] \end{pmatrix}, \quad 9(b)$$

$$\Phi_1[k-1] = \begin{pmatrix} \varphi_{1k}[k-1] \\ \varphi_{2k}[k-1] \end{pmatrix}, \quad (k = 1, 2, \cdots, N). \quad 9(c)$$

Equations (7)-(9) are the recursive formulae of the Nth-order generalized DT for equation (1), which can be applied to obtain rogue wave solutions. In the next section, higher-order rogue wave solutions will be deduced and corresponding dynamics will be depicted and analyzed.

III. ROGUE WAVES SOLUTIONS

We start with a periodic plane seed solution $q[0] = e^{2it}$. The corresponding eigenfunction $\Phi_1(\lambda)$ for equation (2) at $\lambda = -i + \eta^2$ is

$$\Phi_1(\lambda) = \begin{pmatrix} (C_1 e^A + C_2 e^{-A})e^{it} \\ (C_2 e^A + C_1 e^{-A})e^{-it} \end{pmatrix}, \quad (10)$$

where

$$C_1 = \sqrt{i\lambda - \sqrt{-\lambda^2 - 1}}, \quad C_2 = \sqrt{i\lambda + \sqrt{-\lambda^2 - 1}},$$
$$A = \sqrt{-\lambda^2 - 1}(x + \delta t + \Omega(\eta)),$$
$$\delta = 16\lambda^4\varepsilon - 8\varepsilon\lambda^2 + 2\lambda + 6\varepsilon + 1,$$
$$\Omega(\eta) = \sum_{j=1}^{n}(a_j + ib_j)\eta^{2j}, (a_j, b_j \in R).$$

η is a small parameter, $\Omega(\eta)$ is separating function, which contains $2n$ free parameters a_j, $b_j (j = 1, 2, \cdots, n)$ and a_j, b_j are real constants.

Then, expanding $\Phi_1(\lambda)$ at $\eta = 0$ as follows

$$\Phi_1(\eta) = \Phi_1^{[0]} + \Phi_1^{[1]}\eta^2 + \Phi_1^{[2]}\eta^4 + \Phi_1^{[3]}\eta^6 + \cdots + \Phi_1^{[m]}\eta^{2m} + \cdots, \quad (11)$$

with

$$\Phi_1^{[0]} = \begin{pmatrix} 2e^{it} \\ 2e^{-it} \end{pmatrix}, \quad \Phi_1^{[1]} = \begin{pmatrix} \varphi_1^{[1]} \\ \varphi_2^{[1]} \end{pmatrix}, \quad \Phi_1^{[2]} = \begin{pmatrix} \varphi_1^{[2]} \\ \varphi_2^{[2]} \end{pmatrix}, \cdots,$$

and $(\varphi_1^{[i]}, \varphi_2^{[i]})^T, (i = 1, 2)$ are given in the Appendix A.

Substituting $\Phi_1^{[0]}$, $q[0] = e^{2it}$ and $\lambda = -i$ into equations (8) and (9a), we get a trivial solution $q[1] = -e^{2it}$ of equation (1) and

$$T_1[1] = \begin{pmatrix} -i & ie^{2it} \\ ie^{-2it} & -i \end{pmatrix}. \quad (12)$$

Consider the following limit

$$\lim_{\eta\to 0}\frac{[T_1[1]|_{\lambda=\lambda_1+\eta}]\Psi}{\eta} = \lim_{\eta\to 0}\frac{[\eta + T_1[1]|_{\lambda=\lambda_1}]\Psi}{\eta} = \Phi_1^{[0]} + T_1[1](\lambda_1)\Phi_1^{[1]} = \Phi_1[1], \quad (13)$$

where

$$\Phi_1[1] = \begin{pmatrix} \varphi_1[1] \\ \varphi_2[1] \end{pmatrix} = \begin{pmatrix} (4it - 60t\varepsilon - 2t - 2x + 1)e^{it} \\ (-4it + 60t\varepsilon + 2t + 2x + 1)e^{-it} \end{pmatrix}.$$

Then, we obtain the first-order rogue wave solution of equation (1)

$$q[2] = q[1] - 2i\frac{(-2i)\varphi_1[1]\varphi_2^*[1]}{|\varphi_1[1]|^2 + |\varphi_2[1]|^2} = -(1 + 2\frac{F}{G})e^{2it}, \quad (14)$$
$$F = 1 - 20t^2 - 240t\varepsilon x - 3600t^2\varepsilon^2 - 240t^2\varepsilon - 8tx - 4x^2 + 8it,$$
$$G = 20t^2 + 8tx + 240\varepsilon t^2 + 4x^2 + 240t\varepsilon x + 3600t^2\varepsilon^2 + 1.$$

Next, consider the following limit

$$\lim_{\eta\to 0}\frac{[\eta + T_1[2]|_{\lambda=\lambda_1}][\eta + T_1[1]|_{\lambda=\lambda_1}]\Psi}{\eta^2} = \Phi_1^{[0]} + (T_1[1](\lambda_1) + T_1[2](\lambda_1))\Phi_1^{[1]} + T_1[2](\lambda_1)T_1[1](\lambda_1)\Phi_1^{[2]} = \Phi_1[2], \quad (15)$$

where

$$\Phi_1[2] = \begin{pmatrix} \varphi_1[2] \\ \varphi_2[2] \end{pmatrix}$$

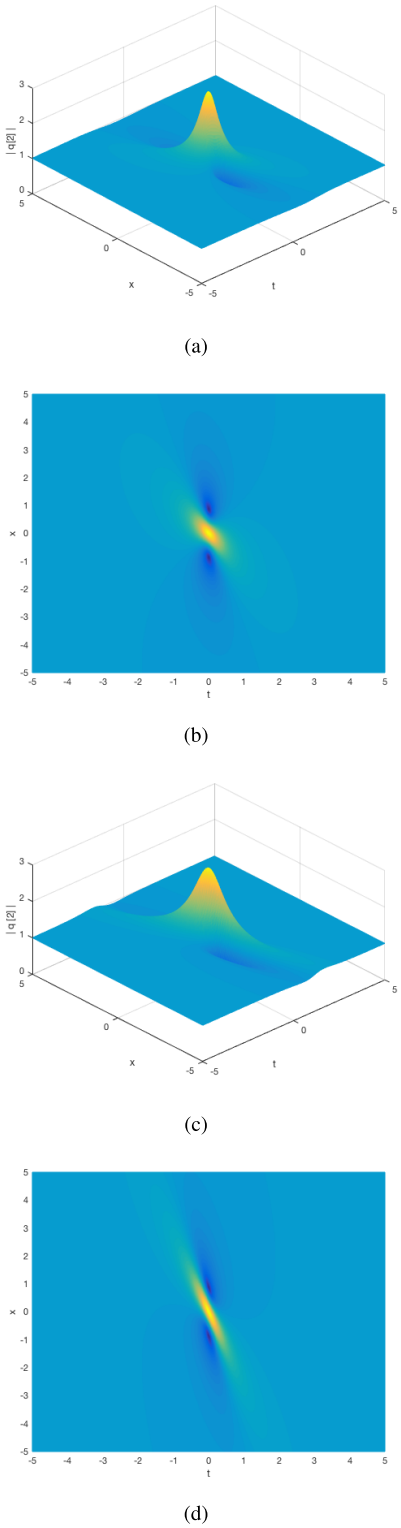

FIGURE 1. Dynamical evolution of the first-order rogue wave (a)-(b) with $\varepsilon = 0$ and (c)-(d) with $\varepsilon = 0.05$.

is given in the Appendix B and $T_1[2]$ is omitted, which can be calculated by Maple. Substituting $\Phi_1[2]$, $q[2]$ and $\lambda = -i$ into equation (8), we get the second-order rogue wave

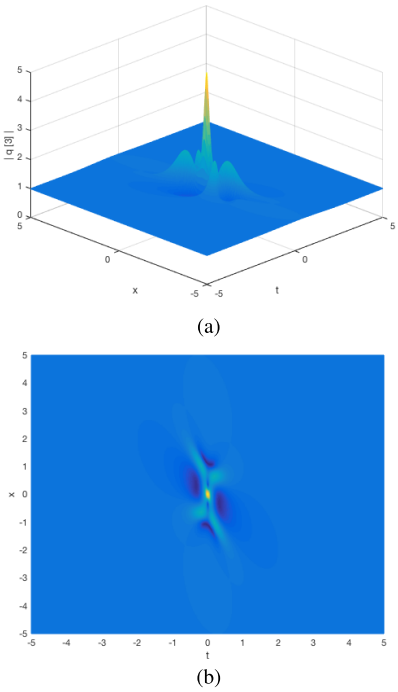

FIGURE 2. Dynamical evolution of the second-order rogue wave with $\varepsilon = 0$, $a_1 = b_1 = 0$.

solution of equation (1)

$$q[3] = q[2] - 2i\frac{(-2i)\varphi_1[2]\varphi_2^*[2]}{|\varphi_1[2]|^2 + |\varphi_2[2]|^2}, \tag{16}$$

which is too cumbersome to work out concretely.

Furthermore, compute the following limitation

$$\begin{aligned}
&\lim_{\eta\to 0}\frac{[\eta + T_1[3]|_{\lambda=\lambda_1}][\eta + T_1[2]|_{\lambda=\lambda_1}][\eta + T_1[1]|_{\lambda=\lambda_1}]\Psi}{\eta^3}\\
&= \Phi_1^{[0]} + (T_1[1](\lambda_1) + T_1[2](\lambda_1) + T_1[3](\lambda_1))\Phi_1^{[1]}\\
&\quad + (T_1[2](\lambda_1)T_1[1](\lambda_1) + T_1[3](\lambda_1)T_1[1](\lambda_1)\\
&\quad + T_1[3](\lambda_1)T_1[2](\lambda_1))\Phi_1^{[2]}\\
&\quad + T_1[3](\lambda_1)T_1[2](\lambda_1)T_1[1](\lambda_1)\Phi_1^{[3]} = \Phi_1[3],
\end{aligned} \tag{17}$$

where

$$\Phi_1[3] = \begin{pmatrix}\varphi_1[3]\\ \varphi_2[3]\end{pmatrix}.$$

$T_1[3]$ can be derived by Maple, which is rather tedious to write down. Substituting $\Phi_1[3]$, $q[3]$ and $\lambda = -i$ into equation (8), we achieve the third-order rogue wave solution

$$q[4] = q[3] - 2i\frac{(-2i)\varphi_1[3]\varphi_2^*[3]}{|\varphi_1[3]|^2 + |\varphi_2[3]|^2}, \tag{18}$$

which is omitted here for it is very prolix.

Carrying on the limitation procedure, we can acquire higher-order rogue wave solutions of equation (1) theoretically. Nevertheless, it is very difficult to gain the expression of $\Phi_1[4]$ by Maple because of complicated calculation.

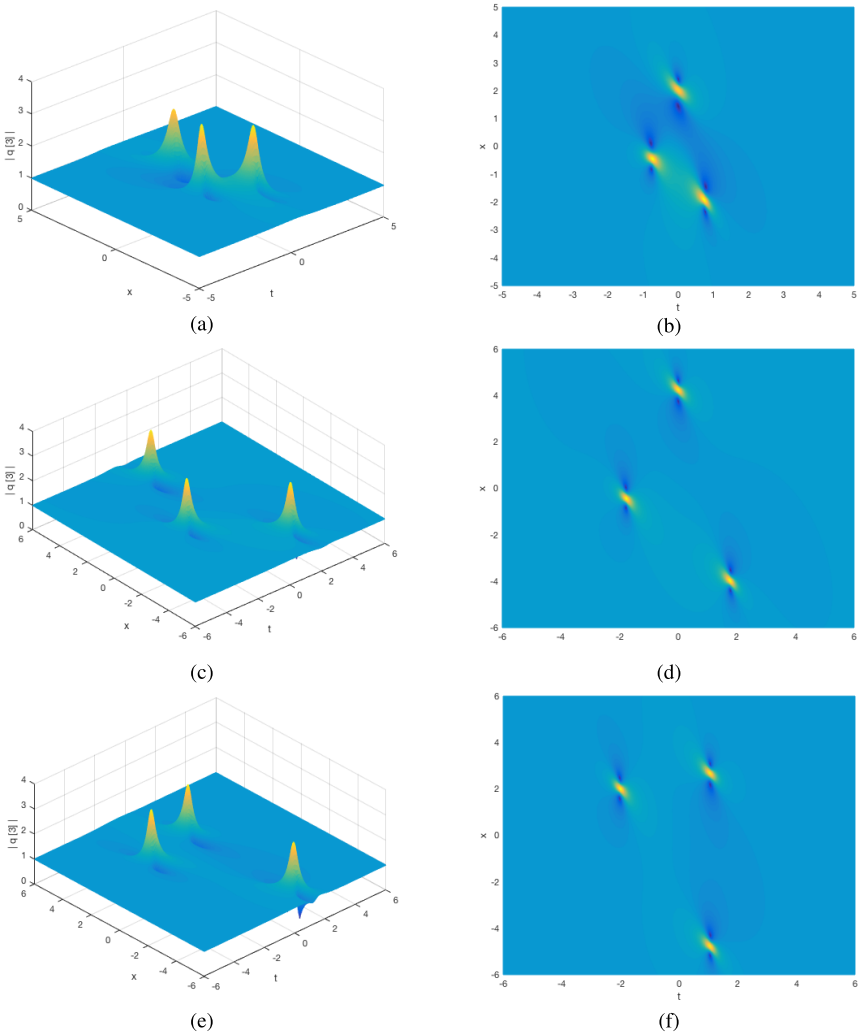

FIGURE 3. Dynamical evolution of the second-order rogue wave (a)-(b) with $b_1 = 5$, (c)-(d) with $b_1 = 50$ and (e)-(f) with $a_1 = 50$.

IV. NUMERICAL SIMULATIONS

On the basis of the rogue wave solutions, nonlinear dynamic properties of higher-order rogue waves to equation (1) are discussed in this section with the help of numerical simulations.

There is only one perturbation parameter ε in equation (14). The 3-dimensional plots and density plots of the first-order rogue wave changing with ε are shown in Figure 1, where the maximum amplitude is 3. The centers of one peak and two valleys lie in the straight line, and the two valleys are symmetric with respect to the peak, as shown in Figure 1(b). It is observed that the compression in t direction is a little high with ε increases and there is no much effect on the pattern of the rogue wave.

There are one perturbation parameter ε and two free parameters a_1 and b_1 in the second-order rogue wave solution. For the specific case $\varepsilon = 0$ and $a_1 = b_1 = 0$, the corresponding 3-dimensional plot and density plot are displayed in Figure 2. It is the fundamental pattern that a highest peak appears at the center and four small peaks surround it in two sides. The maximum amplitude is 5.

Then, we study the influence of two free real parameters a_1 and b_1 on the second-order rogue wave with $\varepsilon = 0$. Upon setting $a_1 = 0$, $b_1 = 5$, the 3-dimensional plots and density plots are depicted in Figures 3(a) and 3(b). It can be seen from the pictures that the fundamental second-order rogue wave is splitted into three first-order ones which form a triangle and the two first-order rogue waves are not separated completely. Increasing the value of b_1, the corresponding plots are given in Figures 3(c) and 3(d) with $b_1 = 50$. It is found easily that three first-order rogue waves are separated completely. In Figures 3(e) and 3(f), $a_1 = 50$, $b_1 = 0$ have been taken. Three first-order rogue waves array an isosceles triangle. Furthermore, it can be verified using numerical simulation that the parameter b_1 plays an

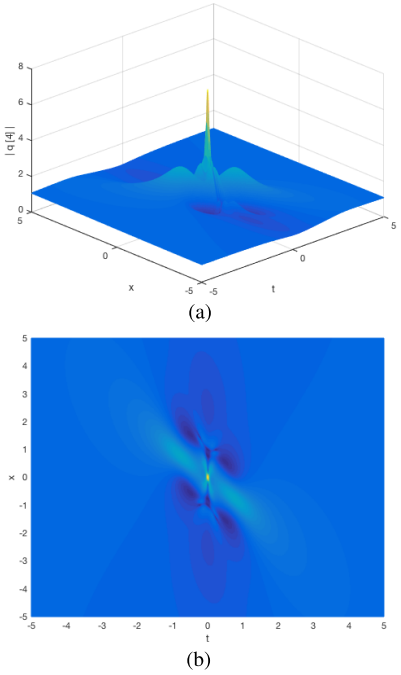

FIGURE 4. Dynamical evolution of the third-order rogue wave with $\varepsilon = 0$, $a_1 = b_1 = 0$ and $a_2 = b_2 = 0$.

important role on the separation and the parameter a_1 can be used to change the position of the three first-order rogue waves.

There are five parameters ε, a_1, b_1, a_2 and b_2 in the third-order rogue wave solution $q[4]$. Upon setting $\varepsilon = 0$, $a_1 = b_1 = 0$ and $a_2 = b_2 = 0$, the corresponding 3-dimensional plot and density plot are demonstrated in Figure 4. Like the second-order rogue wave, it is the fundamental pattern that a highest peak appears at the center and six small peaks surround it. The maximum amplitude is 7.

Keep the other parameters unchanged and suppose $b_1 = 20$, the corresponding 3-dimensional plot and density plot are derived in Figure 5(a) and 5(b). It is clear that the third-order rogue waves are composed of six first-order rogue waves, which form a hexagon pattern. Three of them are big peaks and the others are small ones. Change the parameter $b_2 = 500$, the corresponding plots are given in Figures 5(c) and 5(d). However, it is obviously seen that the six first-order rogue waves array a pentagon. One wave is located in the center and other waves are put on the vertices of the pentagon. Likewise, it can be found with the help of the numerical simulation that there is no much effect on the pattern of the third-order rogue wave if the value of a_1 or a_2 is changed.

With the increase of the order for the rogue wave solution $q[N]$, there are more free parameters, which will array more interesting and novel patterns. It is guessed that these new patterns could be a polygon which could be extended to general the Nth-order systems.

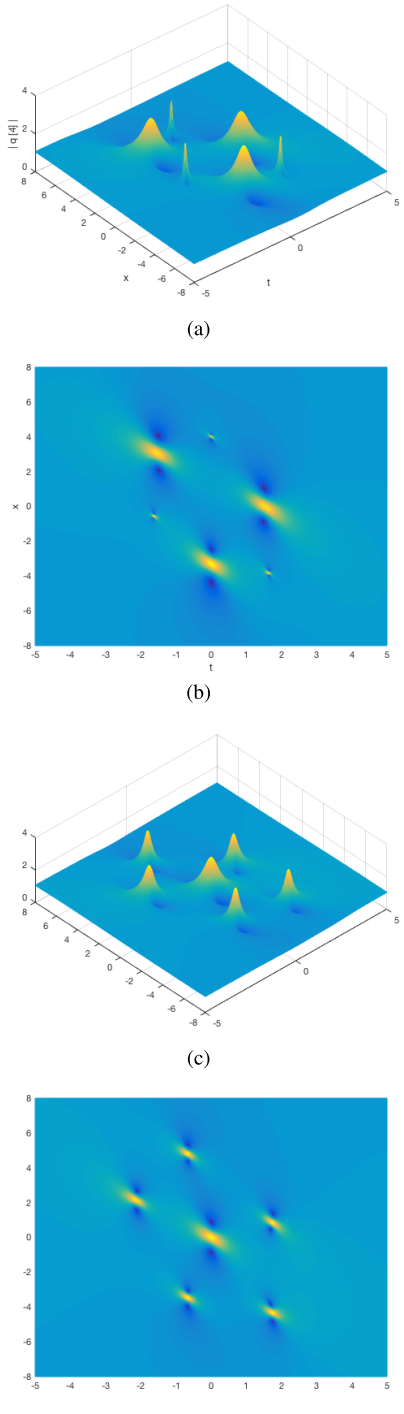

FIGURE 5. Dynamical evolution of the third-order rogue wave (a)-(b) with $b_1 = 20$, (c)-(d) with $b_2 = 500$.

V. CONCLUSION

In this paper, nonlinear dynamics of higher-order rogue waves for the fifth-order nonlinear Schrödinger equation were investigated. On the basis of the Lax pair, the Nth-order rogue waves solutions were derived by using DT, the Taylor expansion and a limit procedure, which contain

$2N-1$ free parameters. Using the numerical simulation, the 3-dimensional plots and density plots of the first-, second- and third-order rogue waves were displayed to illustrate the nonlinearity effect. It can be found that the parameters have a great influence on the array of the rogue waves and there is $\frac{N(N+1)}{2}$ peaks in terms of a complete decomposition pattern. With the increase of the order N, the calculation is more complicated and there will be more interesting plots. We are looking forward to seeing experiments which can verify the theoretical results.

APPENDIXES

APPENDIX A

$$
\begin{aligned}
&\varphi_1^{[1]}\\
&= e^{it}(-6it^2+240\varepsilon t^2+1800i\varepsilon^2t^2+8t^2+8tx+120i\varepsilon t^2\\
&\quad+120i\varepsilon tx+4itx+2ix^2-4t-60i\varepsilon t-2it-2ix+\frac{i}{2}).\\
&\varphi_2^{[1]}\\
&= e^{-it}(-6it^2+240\varepsilon t^2+1800i\varepsilon^2t^2+8t^2+8tx+120i\varepsilon t^2\\
&\quad+120i\varepsilon tx+4itx+2ix^2+4t+60i\varepsilon t+2it+2ix+\frac{i}{2}).\\
&\varphi_1^{[2]}\\
&= e^{it}(\frac{t}{2}+\frac{x}{2}+2b_1+175t\varepsilon+\frac{1}{16}+\frac{7}{3}t^4-\frac{1}{3}x^4\\
&\quad+\frac{2}{3}x^3-\frac{22}{3}t^3+\frac{41}{2}t^2-\frac{3}{2}x^2-8it^4+14it^2+\frac{4}{3}it^3\\
&\quad-5it-4tb_1-4xb_1+8ta_1-2ia_1+18000t^3\varepsilon^3\\
&\quad+1800t^3\varepsilon^2-180t^3\varepsilon-6t^2x+2tx^2+5400\varepsilon^2t^4\\
&\quad+440\varepsilon t^4+\frac{44}{3}t^3\varepsilon+6t^2x^2-\frac{4}{3}tx^3-270000\varepsilon^4t^4\\
&\quad-36000\varepsilon^3t^4-410\varepsilon t^2-3tx-10950\varepsilon^2t^2-4itx^2\\
&\quad+120i\varepsilon ta_1+7200i\varepsilon^2t^3x+480i\varepsilon t^3x+240i\varepsilon t^2x^2\\
&\quad-240i\varepsilon t^2x+14itx-120\varepsilon tb_1+8itb_1+72000i\varepsilon^3t^4\\
&\quad+7200i\varepsilon^2t^4+8it^2x^2+\frac{8}{3}itx^3+4ita_1+4ixa_1-240i\varepsilon t^3\\
&\quad-3600i\varepsilon^2t^3-8it^2x-80i\varepsilon t^4-\frac{8}{3}it^3x+1060i\varepsilon t^2\\
&\quad-36000\varepsilon^3t^3x-1800\varepsilon^2t^2x^2+360\varepsilon t^3x-120\varepsilon t^2x^2\\
&\quad-40\varepsilon tx^3+1800\varepsilon^2t^2x+120\varepsilon t^2x+60\varepsilon tx^3-410\varepsilon tx).\\
&\varphi_2^{[2]}\\
&= e^{-it}(-\frac{t}{2}-\frac{x}{2}-2b_1-175t\varepsilon+\frac{1}{16}+\frac{7}{3}t^4-\frac{1}{3}x^4\\
&\quad-\frac{2}{3}x^3+\frac{22}{3}t^3+\frac{41}{2}t^2-\frac{3}{2}x^2-8it^4+14it^2-\frac{4}{3}it^3\\
&\quad+5it-4tb_1-4xb_1+8ta_1+2ia_1-18000t^3\varepsilon^3\\
&\quad-1800t^3\varepsilon^2+180t^3\varepsilon+6t^2x-2tx^2+5400\varepsilon^2t^4\\
&\quad+440\varepsilon t^4+\frac{44}{3}t^3\varepsilon+6t^2x^2-\frac{4}{3}tx^3-270000\varepsilon^4t^4\\
&\quad-36000\varepsilon^3t^4-410\varepsilon t^2-3tx-10950\varepsilon^2t^2+4itx^2\\
&\quad+120i\varepsilon ta_1+7200i\varepsilon^2t^3x+480i\varepsilon t^3x+240i\varepsilon t^2x^2\\
&\quad+240i\varepsilon t^2x+14itx-120\varepsilon tb_1+8itb_1+72000i\varepsilon^3t^4\\
&\quad+7200i\varepsilon^2t^4+8it^2x^2+\frac{8}{3}itx^3+4ita_1+4ixa_1+240i\varepsilon t^3\\
&\quad+3600i\varepsilon^2t^3+8it^2x-80i\varepsilon t^4-\frac{8}{3}it^3x+1060i\varepsilon t^2\\
&\quad-36000\varepsilon^3t^3x-1800\varepsilon^2t^2x^2+360\varepsilon t^3x-120\varepsilon t^2x^2\\
&\quad-40\varepsilon tx^3-1800\varepsilon^2t^2x-120\varepsilon t^2x-60\varepsilon tx^3-410\varepsilon tx).
\end{aligned}
$$

APPENDIX B

$$
\begin{aligned}
&\varphi_1[2]\\
&= -\frac{1}{3}\frac{1}{\Delta}e^{it}(-3+18t+18x+96it^2x+480t^4\\
&\quad-32x^4+296t^3+8x^3+252t^2+12x^2+21600\varepsilon^2t^3\\
&\quad+9360\varepsilon t^3+312t^2x+24tx^2+48tb_1+48xb_1+96ta_1\\
&\quad-25920000\varepsilon^4t^4-3456000\varepsilon^3t^4-172800\varepsilon^2t^4\\
&\quad-3840\varepsilon t^4-128t^3x-192t^2x^2+216000\varepsilon^3t^3\\
&\quad+126000\varepsilon^2t^2-128tx^3+4560\varepsilon t^2+24tx\\
&\quad-3456000\varepsilon^3t^3x-345600\varepsilon^2t^3x-172800\varepsilon^2t^2x^2\\
&\quad-11520\varepsilon^3x+21600\varepsilon^2t^2x-11520\varepsilon t^2x^2-3840\varepsilon tx^3\\
&\quad+1440\varepsilon t^2x+720\varepsilon tx^2+1440\varepsilon tb_1+4560\varepsilon tx\\
&\quad+640it^4-96it^2+2880i\varepsilon t^2x+345600i\varepsilon^2t^3x\\
&\quad+23040i\varepsilon t^3x+11520i\varepsilon t^2x^2-1440i\varepsilon ta_1+2460\varepsilon t\\
&\quad-272it^3-84it+3456000i\varepsilon^3t^4+345600i\varepsilon^2t^4\\
&\quad+26880i\varepsilon t^4+896it^3x+384it^2x^2+128itx^3\\
&\quad+4800i\varepsilon t^2-96itx-48ita_1+96itb_1-48ixa_1\\
&\quad+24b_1-24ia_1+43200i\varepsilon^2t^3+2880i\varepsilon t^3+48itx^2).\\
&\varphi_2[2]\\
&= -\frac{1}{3}\frac{1}{\Delta}e^{-it}(-3-18t-18x-96it^2x+480t^4\\
&\quad-32x^4-296t^3-8x^3+252t^2+12x^2-21600\varepsilon^2t^3\\
&\quad-9360\varepsilon t^3-312t^2x-24tx^2+48tb_1+48xb_1+96ta_1\\
&\quad-25920000\varepsilon^4t^4-3456000\varepsilon^3t^4-172800\varepsilon^2t^4\\
&\quad-3840\varepsilon t^4-128t^3x-192t^2x^2-216000\varepsilon^3t^3\\
&\quad+126000\varepsilon^2t^2-128tx^3+4560\varepsilon t^2+24tx\\
&\quad-3456000\varepsilon^3t^3x-345600\varepsilon^2t^3x-172800\varepsilon^2t^2x^2\\
&\quad-11520\varepsilon^3x-21600\varepsilon^2t^2x-11520\varepsilon t^2x^2-3840\varepsilon tx^3\\
&\quad-1440\varepsilon t^2x-720\varepsilon tx^2+1440\varepsilon tb_1+4560\varepsilon tx\\
&\quad+640it^4-96it^2-2880i\varepsilon t^2x+345600i\varepsilon^2t^3x\\
&\quad+23040i\varepsilon t^3x+11520i\varepsilon t^2x^2-1440i\varepsilon ta_1-2460\varepsilon t\\
&\quad+272it^3+84it+3456000i\varepsilon^3t^4+345600i\varepsilon^2t^4\\
&\quad+26880i\varepsilon t^4+896it^3x+384it^2x^2+128itx^3\\
&\quad+4800i\varepsilon t^2-96itx-48ita_1+96itb_1-48ixa_1\\
&\quad-24b_1+24ia_1-43200i\varepsilon^2t^3-2880i\varepsilon t^3-48itx^2).\\
&\Delta = 3600\varepsilon^2t^2+240\varepsilon t^2+240\varepsilon tx+20t^2+8tx+4x^2+1.
\end{aligned}
$$

REFERENCES

[1] P. Müller, C. Garrett, and A. Osborne, "Rogue waves," *Oceanography*, vol. 18, no. 3, pp. 66–75, 2005.

[2] G. Genty, J. M. Dudley, and B. J. Eggleton, "Modulation control and spectral shaping of optical fiber supercontinuum generation in the picosecond regime," *Appl. Phys. B, Lasers Opt.*, vol. 94, no. 2, pp. 187–194, Feb. 2009.
[3] G. Genty, C. De Sterke, O. Bang, F. Dias, N. Akhmediev, and J. Dudley, "Collisions and turbulence in optical rogue wave formation," *Phys. Lett. A*, vol. 374, no. 7, pp. 989–996, Feb. 2010.
[4] D. I. Yeom and B. J. Eggleton, "Photonics: Rogue waves surface in light," *Nature*, vol. 450, pp. 953–954, Dec. 2007.
[5] W. M. Moslem, P. K. Shukla, and B. Eliasson, "Surface plasma rogue waves," *Europhys. Lett. Assoc.*, vol. 96, no. 2, Oct. 2011, Art. no. 25002.
[6] V. Efimov, A. Ganshin, G. Kolmakov, P. Mcclintock, and L. Mezhov-Deglin, "Rogue waves in superfluid helium," *Eur. Phys. J. Special Topics*, vol. 185, no. 1, pp. 181–193, Jul. 2010.
[7] M. Shats, H. Punzmann, and H. Xia, "Capillary rogue waves," *Phys. Rev. Lett.*, vol. 104, Mar. 2011, Art. no. 104503.
[8] *Rogue Waves: Monsters of the Deep*, The Economist, Westminster, U.K., 2009, vol. 7.
[9] H. Johnston, "Freak waves spotted from space," BBC News, May 2010.
[10] A. Benetazzo, F. Barbariol, F. Bergamasco, A. Torsello, S. Carniel, and M. Sclavo, "Observation of extreme sea waves in a space-time ensemble," *J. Phys. Oceanogr.*, vol. 45, no. 9, pp. 2261–2275, Sep. 2015.
[11] P. C. Liu, A. V. Babanin, K. R. MacHutchon, and N. Mori, "Rogue waves and explorations of coastal wave characteristic," Glerl. Noaa. Gov., Sep. 2018.
[12] N. Bigaouette, E. Ackad, and L. Ramunno, "Nonlinear grid mapping applied to an FDTD-based, multi-center 3D Schrödinger equation solver," *Comput. Phys. Commun.*, vol. 183, no. 1, pp. 38–45, Jan. 2012.
[13] X.-F. Pang, "The dynamic natures of microscopic particles described by nonlinear Schrödinger equation," *Phys. B, Condens. Matter*, vol. 404, no. 16, pp. 2353–2358, Aug. 2009.
[14] D. H. Peregrine, "Water waves, nonlinear Schrödinger equations and their solutions," *J. Austral. Math. Soc.*, vol. 25, pp. 16–43, Jul. 1983.
[15] N. Akhmediev, A. Ankiewicz, and J. M. Soto-Crespo, "Rogue waves and rational solutions of the nonlinear Schrödinger equation," *Phys. Rev. E, Stat. Phys. Plasmas Fluids Relat. Interdiscip. Top.*, vol. 80, Aug. 2009, Art. no. 026601.
[16] H.-P. Zhu, "Nonlinear tunneling for controllable rogue waves in two dimensional graded-index waveguides," *Nonlinear Dyn.*, vol. 72, no. 4, pp. 873–882, Jun. 2013.
[17] Q. L. Zha, "On Nth-order rogue wave solution to the generalized nonlinear Schrödinger equation," *Phys. Lett. A*, vol. 377, no. 12, pp. 855–859, May 2013.
[18] W.-Q. Peng, S.-F. Tian, X.-B. Wang, T.-T. Zhang, and Y. Fang, "Riemann–Hilbert method and multi-soliton solutions for three-component coupled nonlinear Schrödinger equations," *J. Geometry Phys.*, vol. 146, Dec. 2019, Art. no. 103508.
[19] X. W. Yan, S. F. Tian, M. J. Dong, and T. T. Zhang, "Rogue waves and their dynamics on bright-dark soliton background of the coupled higher order nonlinear Schrödinger equation," *J. Phys. Soc. Jpn.*, vol. 88, Jun. 2019, Art. no. 074004.
[20] D. Guo, S.-F. Tian, and T.-T. Zhang, "Integrability, soliton solutions and modulation instability analysis of a(2+1)-dimensional nonlinear Heisenberg ferromagnetic spin chain equation," *Comput. Math. Appl.*, vol. 77, no. 3, pp. 770–778, Feb. 2019.
[21] S. F. Tian, "Initial-boundary value problems for the general coupled nonlinear Schrödinger equation on the interval via the Fokas method," *J. Differ. Equ.*, vol. 262, pp. 506–558, Jan. 2017.
[22] F. Sh Tian, "The mixed coupled nonlinear Schrödinger equation on the half-line via the Fokas method," *Roy. Soc. A*, vol. 472, p. 0588, Nov. 2016.
[23] W. Q. Peng, S. F. Tian, and T. T. Zhang, "Dynamics of breather waves and higher-order rogue waves in a coupled nonlinear Schrödinger equation," *Lett. J. Exploring Frontiers Phys.*, vol. 123, Oct. 2018.
[24] W. Q. Peng, S. F. Tian, and T. T. Zhang, "Breather waves, high-order rogue waves and their dynamics in the coupled nonlinear Schrödinger equations with alternate signs of nonlinearities," *Lett. J. Exploring Frontiers Phys.*, vol. 127, Oct. 2019, Art. no. 50005.
[25] S.-F. Tian and T.-T. Zhang, "Long-time asymptotic behavior for the Gerdjikov-Ivanov type of derivative nonlinear Schrödinger equation with time-periodic boundary condition," *Proc. Amer. Math. Soc.*, vol. 146, no. 4, pp. 1713–1729, Dec. 2017.
[26] A. Ankiewicz, J. M. Soto-Crespo, and N. Akhmediev, "Rogue waves and rational solutions of the Hirota equation," *Phys. Rev. E, Stat. Phys. Plasmas Fluids Relat. Interdiscip. Top.*, vol. 81, Apr. 2010, Art. no. 046602.
[27] J. He, S. Xu, and K. Porsezian, "Rogue waves of the Fokas-Lenells equation," *J. Phys. Soc. Jpn.*, vol. 81, no. 12, Dec. 2012, Art. no. 124007.
[28] U. Bandelow and N. Akhmediev, "Sasa-Satsuma equation: Soliton on a background and its limiting cases," *Phys. Rev. E, Stat. Phys. Plasmas Fluids Relat. Interdiscip. Top.*, vol. 86, Aug. 2012, Art. no. 026606.
[29] A. Ankiewicz, N. Akhmediev, and J. M. Soto-Crespo, "Discrete rogue waves of the Ablowitz-Ladik and Hirota equations," *Phys. Rev. E, Stat. Phys. Plasmas Fluids Relat. Interdiscip. Top.*, vol. 82, Aug. 2010, Art. no. 026606.
[30] C. Z. Li, J. S. He, and K. Porsezian, "Rogue waves of the Hirota Maxwell-Bloch equations," *Phys. Rev. E, Stat. Phys. Plasmas Fluids Relat. Interdiscip. Top.*, vol. 87, Jan. 2013, Art. no. 012913.
[31] J. He, S. Xu, and K. Porsezian, "New types of rogue wave in an erbium-doped fibre system," *J. Phys. Soc. Jpn.*, vol. 81, no. 3, Mar. 2012, Art. no. 033002.
[32] R. Radha and V. R. Kumar, "Explode-decay solitons in the generalized inhomogeneous higher-order nonlinear Schrödinger equations," *Zeitschrift für Naturforschung A*, vol. 62, nos. 7–8, pp. 381–386, Aug. 2007.
[33] H. T. Tchokouansi, V. K. Kuetche, and T. C. Kofane, "On the propagation of solitons in ferrites: The inverse scattering approach," *Chaos, Solitons Fractals*, vol. 86, pp. 64–74, May 2016.
[34] B.-Q. Li and Y.-L. Ma, "Loop-like periodic waves and solitons to the Kraenkel-Manna-Merle system in ferrites," *J. Electromagn. Waves Appl.*, vol. 32, no. 10, pp. 1275–1286, Jul. 2018.
[35] M. Tanaka, S. Ohya, and P. N. Hai, "Recent progress in III-V based ferromagnetic semiconductors: Band structure, Fermi level, and tunneling transport," *Appl. Phys. Rev.*, vol. 1, no. 1, Mar. 2014, Art. no. 011102.
[36] B. K. Esbensen, A. Wlotzka, M. Bache, O. Bang, and W. Krolikowski, "Modulational instability and solitons in nonlocal media with competing nonlinearities," *Phys. Rev. A, Gen. Phys.*, vol. 84, Nov. 2011, Art. no. 053854.
[37] H.-Q. Zhang, B. Tian, X.-H. Meng, X. Lü, and W.-J. Liu, "Conservation laws, soliton solutions and modulational instability for the higher-order dispersive nonlinear Schrödinger equation," *Eur. Phys. J. B*, vol. 72, no. 2, pp. 233–239, Nov. 2009.
[38] W.-Q. Peng, S.-F. Tian, and T.-T. Zhang, "Dynamics of the soliton waves, breather waves, and rogue waves to the cylindrical Kadomtsev-Petviashvili equation in pair-ion-electron plasma," *Phys. Fluids*, vol. 31, no. 10, Oct. 2019, Art. no. 102107.
[39] C.-Y. Qin, S.-F. Tian, X.-B. Wang, T.-T. Zhang, and J. Li, "Rogue waves, bright-dark solitons and traveling wave solutions of the (3+1)-dimensional generalized Kadomtsev-Petviashvili equation," *Comput. Math. Appl.*, vol. 75, no. 12, pp. 4221–4231, Jun. 2018.
[40] W.-Q. Peng, S.-F. Tian, and T.-T. Zhang, "Breather waves and rational solutions in the (3+1)-dimensional Boiti-Leon-Manna-Pempinelli equation," *Comput. Math. Appl.*, vol. 77, no. 3, pp. 715–723, Feb. 2019.
[41] C. Y. Yang, W. Liu, Q. Zhou, D. Mihalache, and B. A. Malomed, "One-soliton shaping and two-soliton interaction in the fifth-order variable-coefficient nonlinear Schrödinger equation," *Nonlinear Dyn.*, vol. 95, no. 1, pp. 369–380, Jan. 2019.
[42] W. R. Sun, B. Tian, H. L. Zhen, and Y. Sun, "Breathers and rogue waves of the fifth-order nonlinear Schrödinger equation in the Heisenberg ferromagnetic spin chain," *Nonlinear Dyn.*, vol. 81, pp. 725–732, Jul. 2015.
[43] N. Song, W. Zhang, and M. H. Yao, "Complex nonlinearities of rogue waves in generalized inhomogeneous higher-order nonlinear Schrödinger equation," *Nonlinear Dyn.*, vol. 82, nos. 1–2, pp. 489–500, Oct. 2015.
[44] M. Wang, W. R. Shan, B. Tian, and Z. Tan, "Darboux transformation and conservation laws for an inhomogeneous fifth-order nonlinear Schrödinger equation from the Heisenberg ferromagnetism," *Commun. Nonlinear Sci. Numer. Simul.*, vol. 20, pp. 692–698, Mar. 2015.
[45] Z. Zhao and L. He, "Multiple lump solutions of the (3+1)-dimensional potential Yu-Toda-Sasa-Fukuyama equation," *Appl. Math. Lett.*, vol. 95, pp. 114–121, Sep. 2019.
[46] X. B. Wang and B. Han, "The three-component coupled nonlinear Schrödinger equation: Rogue waves on a multi-soliton background and dynamics," *Lett. J. Exploring Frontiers Phys.*, vol. 126, no. 1, 2019, Art. no. 15001.
[47] X.-B. Wang, S.-F. Tian, L.-L. Feng, and T.-T. Zhang, "On quasi-periodic waves and rogue waves to the (4+1)-dimensional nonlinear Fokas equation," *J. Math. Phys.*, vol. 59, no. 7, Jul. 2018, Art. no. 073505.

[48] X. B. Wang, S. F. Tian, and T. T. Zhang, "Characteristics of the breather and rogue waves in a (2+1)-dimensional nonlinear Schrödinger equation," *Proc. Amer. Math. Soc.*, vol. 146, no. 8, pp. 3353–3365, 2018.
[49] B. L. Guo, L. M. Ling, and Q. P. Liu, "Nonlinear Schrödinger equation: Generalized Darboux transformation and rogue wave solutions," *Phys. Rev. E, Stat. Phys. Plasmas Fluids Relat. Interdiscip. Top.*, vol. 85, Feb. 2012, Art. no. 026607.

NI SONG was born in Shanxi, China, in 1979. She received the Ph.D. degree from the Beijing University of Technology, Beijing, China, in 2015. She is currently an Associate Professor and a Master Tutor with the Department of Mathematics, North University of China, Shanxi, China. Her research interests include dynamics systems and nonlinear analysis fields.

HUI XUE was born in Shanxi, China, in 1994. She received the bachelor's degree from the Department of Mathematics, Taiyuan Normal University, Shanxi, in 2017. She is currently pursuing the master's degree with the Department of Mathematics, School of Science, North University of China, Shanxi. Her research interest includes nonlinear analysis and application.

XIAOYING ZHAO was born in Shanxi, China, in 1995. She received the bachelor's degree from the Department of Mathematics, Changzhi University, Shanxi. She is currently pursuing the master's degree with the Department of Mathematics, School of Science, North University of China, Shanxi. Her research interest includes nonlinear analysis and application.